

Gaussian and q-Gaussian Functions for the Decomposition of J1022+1001 Pulsar Profiles

Original

Gaussian and q-Gaussian Functions for the Decomposition of J1022+1001 Pulsar Profiles / Sparavigna, A. C.. - In: INTERNATIONAL JOURNAL OF SCIENCES. - ISSN 2305-3925. - ELETTRONICO. - 13:6(2024), pp. 18-27. [10.18483/ijSci.2772]

Availability:

This version is available at: 11583/2989560 since: 2024-06-15T11:48:01Z

Publisher:

Alkhaer Publications

Published

DOI:10.18483/ijSci.2772

Terms of use:

This article is made available under terms and conditions as specified in the corresponding bibliographic description in the repository

Publisher copyright

(Article begins on next page)

Gaussian and q-Gaussian Functions for the Decomposition of J1022+1001 Pulsar Profiles

Amelia Carolina Sparavigna¹

¹Department of Applied Science and Technology, Polytechnic University of Turin, Italy

Abstract: The pulsar profiles are profiles obtained by pulse sequences averaged on several cycles. The mean profiles are usually decomposed in Gaussian components, but decompositions in von Mises functions have been proposed too. The Gaussian decompositions can be based on the central limit theorem (CLT), so that a Gaussian component can be regarded as an attractor in the space of distributions with finite variance. Well-known non-Gaussian attractors exist and are the Lévy distributions. Other proposed attractors are the q-Gaussian functions, which are generalizing the Gaussians in the Tsallis q-statistics. These functions have power-law tails. For parameter q equal to 1, the q-Gaussians become the standard Gaussian distributions. In this framework of Gaussian and non-Gaussian attractors, we propose decompositions of pulsar profiles both in Gaussian and q-Gaussian functions. Our investigation is aiming to compare the decompositions to highlight possible differences and dependences on q-parameters. Here we consider, in particular, the intensity profiles given by the EPN Database of Pulsar Profiles, of J1022+1001 at several frequencies. Power-law behaviors of the leading edges have been observed.

Keywords: Pulsar Profiles, Profile Decomposition, q-Gaussian Tsallis Lines, Central Limit Theorem

Introduction

The pulsar profiles, such as those available from the European Pulsar Network (EPN) Database, are profiles obtained by pulse sequences averaged on several cycles. The mean profiles are usually decomposed in Gaussian components. In Wahl et al., 2023, for instance, we can find several examples of such decompositions. The Gaussian fitting procedure used by Wahl and coworkers was made according to Kramer, 1994, and Kramer et al., 1994. Besides Gaussians, the averaged profiles have been fitted to von Mises functions too, as in the work by Van der Wateren and coworkers, 2023. The von Mises distribution is also known as “circular normal distribution” and it is a special case of the von Mises–Fisher distributions. At the basis of these decomposition, there is the general assumption that “the summation of many hundreds or thousands of pulses leads to a stable pulse profile that is characteristic of the pulsar” (Osłowski et al., 2011, mentioning Helfand, Manchester & Taylor 1975). Moreover, “regardless of the original distribution, after a large number of pulses have been integrated, the central limit theorem applies and profile shape variations are well described by a multivariate normal distribution” (Osłowski et al., 2011).

The use of the Gaussian approximation is common in the observations of spectral lines, where data are typically fitted to simplified models. Also in this case, “the central limit theorem suggests that ... the shape of the observed spectrum approaches a Gaussian” (Juvela and Tharakkal, 2024). However, as stressed by Juvela and Tharakkal, “the observed spectra are rarely precisely Gaussian, and they can show asymmetries”, and contain distinct components. “The complexity is often addressed by fitting multiple

Gaussians, ... the sum of the fitted components approximates the observed line profile, and such multi-component fits can be used simply as a tool to estimate [relevant] quantities” (Juvela and Tharakkal, 2024). In the case of the pulsar profiles, where the suggested approximation is the use of a mixture distribution of Gaussians, the presence of asymmetry had been stressed too (Dyks, 2017, “The profiles are often highly asymmetric and have components with flux ratio which curiously evolves with frequency”).

According to the central limit theorem (CLT), the Gaussian functions are attractors in the space of distributions with finite variance. Besides the Gaussian attractors, the well-known Lévy distributions exist. Other proposed attractors are the q-Gaussian functions, which are generalizing the Gaussians in the Tsallis q-statistics. These functions have power-law tails. For parameter q equal to 1, the q-Gaussians become the standard Gaussian distributions. In this framework of Gaussian and non-Gaussian attractors, here we propose decompositions of pulsar profiles both in Gaussian and q-Gaussian functions. The aim is that of comparing the decompositions to highlight possible differences and dependences on q-parameters.

Gaussians on lines and circles

According to the *standard* central limit theorem, the attractor in the distribution space is a Gaussian (Marsh et al., 2006). As told by Marsh and coworkers, “for *independent* systems, the attractor in probability space is a Gaussian, as studied by A. de Moivre (1733), P.S. de Laplace (1774), R. Adrain (1808) and C.F. Gauss (1809), when the variance of the single distribution is finite. If this variance diverges instead, the attractor is a Levy distribution, as studied by P.



Lévy and B.V. Gnedenko in the 1930's" (Marsh et al., 2006; about the Lévy-Gnedenko limit theorem see Bianucci, 2021). Marsh and coworkers continue saying that, "in the anomalous case (i.e., when global correlations are present), a variety of attractors have been conjectured or discussed, most notably the q-Gaussian distribution. This distribution optimizes the entropy S_q [Tsallis entropy]" (Marsh et al., 2006, and references therein). The q-Gaussians are based on the q-exponential functions, proposed by Constantino Tsallis in 1988 for his generalization of Boltzmann-Gibb statistics. As previously told, when the value of the q parameter goes to 1, the q-Gaussian becomes a Gaussian. Moreover, if the q-parameter is less than 5/3, the variance of the distribution is finite.

In 2006, Marsh and coworkers told that "a formal development of a q-generalized Central Limit Theorem (q-CLT) [was] in progress". In 2008, Umarov et al. proposed a q-modified CLT. In this theorem, the constraint for the independent and identically distributed (i.i.d.) variables is modified according to the q-calculus. The independence is recovered as $q \rightarrow 1$. This proof of the q-modified central limit theorem has been questioned by Hilhorst, 2010. In 2011, C. Tsallis answered Hilhorst's observations. In any case, we have mentioned before the Lévy distribution as an attractor. According to the work by Deng, 2010, the q-Gaussian functions are mimicking the Lévy functions in a very good manner (Sparavigna, 2023), and therefore we could consider the q-Gaussians as approximations of Lévy attractors. Let us stress that a q-Gaussian becomes a Gaussian attractor when the value of the q-parameter is close to 1. Let us also note that the Lévy distribution has an infinite variance, whereas the variance of the q-Gaussian distribution is finite if q-parameter is less of 5/3.

In Mantegna and Stanley, 1999, we can find the Gaussian distribution defined as an attractor in the functional space of pdfs (probability distribution functions). "The Gaussian distribution is a peculiar stable distribution; it is the only stable distribution having all its moments finite. It is then natural to ask if non-Gaussian stable distributions are also attractors in the functional space of pdfs. The answer is affirmative" [see discussion in Mantegna and Stanley], according to the Lévy-Gnedenko theorem. As concluded by Mantegna and Stanley, we have an infinite number of attractors in the functional space of pdfs. These attractors "comprise the set of all the stable distributions". In the Figure 4.1 of the book by Mantegna and Stanley, we can see schematically some attractors and their convergences. "An important difference is observed between the Gaussian attractor and the stable non-Gaussian attractors: finite variance random variables are present in the Gaussian basin of attraction, whereas random variables with infinite variance are present in basins of attraction of stable non-Gaussian distributions" (Mantegna & Stanley, 1999).

"Stochastic processes with infinite variance are characterized by distributions with power-law tails. Hence such distributions with power-law tails are present in the stable non-Gaussian basins of attraction" (Mantegna & Stanley, 1999). It is important to note again that the q-Gaussian has a power-law tail, but for $q < 5/3$ the variance is finite.

In Hilhorst, 2009, we can find the discussion of the symmetric and asymmetric Lévy cases. Being $L_{\alpha,\beta}$ the general Lévy distribution, when β is equal to zero we have the symmetric Lévy function, so that when α is one, the Lorentz-Cauchy case is obtained and when α is two, the Gaussian case is obtained. Hilhorst tells that, in the Limit Theorem, "the Gaussian is an attractor under addition of independent identically distributed random variables ... [The] Lévy distributions are attractors under addition of random variables, just like the Gaussian, and each has its own basin of attraction". "Mathematicians tell us that there do not exist any other attractors, at least not for sums of independent identically distributed (i.i.d.) variables. However, suppose you add independent but non-identical variables. If they're not too nonidentical, you still get Gauss and Lévy distributions". To have a Gaussian, we need a condition which is known as the Lindeberg condition. In the case that the Lindeberg condition does not hold, we have a bell-shaped distribution which is neither Gaussian nor Lévy, "but something in between" (Hilhorst, 2009).

Both Lévy, Gaussians and q-Gaussians are distributions on the straight line. In the case of the pulsar profiles, we are on a circle, characterized by phases. Let us write the Gaussian as $\exp(-\kappa x^2/2)$, as it appears in Breitenberger, 1963, in his work about the analogues of the Normal Distribution on the Circle and the Sphere. Regarding the Gaussian on a straight line, Breitenberger tells that it is encountered in a variety of problems; "when analogous problems are formulated on the circle, they assume different complexions. Take the central limit theorem: on the circle the addition of random variables (Lévy, 1939) leads to the uniform distribution (called 'isotropic' by physicists and astronomers). ... Brownian motion on the circle ... leads to a 'wrapped-up normal' distribution, of the type $\sum_n \exp[-(x - 2n\pi)^2/2\sigma^2]$ " (Breitenberger, 1963). Breitenberger also notes that "the normal distribution has several defining properties involving a mean or variance; hence it must have various analogues on circle and sphere, according to the substitutes for mean and variance which one can invent." Being γ an azimuth, von Mises (1918) obtained the distribution $\exp[\kappa \cos(x - \gamma)]$ with κ positive. After being normalized, and with a central polar axis, the distribution is $\exp(\kappa \cos x)/2\pi I_0(\kappa)$, where x is the polar angle and I_0 the modified Bessel function of the first kind. This is the von Mises distribution. In it, κ is the concentration parameter. If

the distribution is highly concentrated, we can neglect the circularity and approximate the von-Mises distribution as normal.

The q-Gaussians

Returning to the q-Gaussian functions, (Tsallis, 1988, Umarov et al., 2008, Hanel et al., 2009), they are given as $f(x) = Ce_q(-\beta x^2)$, where $e_q(\cdot)$ is the q-exponential function and C a constant (in the exponent, $\beta = 1/(2\sigma^2)$). The q-exponential has expression: $e_q(u) = [1 + (1 - q)u]^{1/(1-q)}$ (q is continuous real parameter). When q is going to 1, the q-exponential becomes the usual exponential function. The value $q=2$, (Naudts, 2009), corresponds to the Cauchy distribution, also known as the Lorentzian distribution. The change of q-parameter is allowing the q-Gaussian function to pass from the Gaussian to the Lorentzian distribution. In fact, we are passing from a distribution with a finite variance, when q is less than $5/3$, to a distribution with infinite variance, for q equal or greater than $5/3$ and lower than 2. In a [previous discussion about decompositions](#) of pulsar profiles, we have found cases where the q-Gaussians and their asymmetric versions can give very good results. However, is it better to use, for the pulsar profiles, a Gaussian or a non-Gaussian shape?

The tails

In Kramer et al., 1994, the studied profiles are decomposed in a sum of Gaussians. “The assumption that single components in the pulsar profiles can be best represented by a Gaussian shape has been made by several authors”. Among them we find Krishnamohan and Downs, 1983. In this mentioned research, we can find told that “The observed change of the pulse profile with the intensity (Fig. 5 in Krishnamohan and Downs) suggests that there are several independently varying components present in the emission of [the studied] pulsar [Vela, PSR 0833 — 45]. The spectral features discussed in § IIIb [by Krishnamohan and Downs], lend support to this hypothesis. Furthermore, the average pulse profile of this pulsar changes markedly with frequency, as do the profiles of many other pulsars”. “To decompose the pulse profiles, we need to know the shapes expected for the components. Unfortunately, an examination of strong individual pulses did not show any pulses that have only one component. The manner in which the trailing and the leading edges approached the baseline suggested that a Gaussian shape may be a *good approximation for the average shape of each component*” (Krishnamohan and Downs, 1983). Krishnamohan and Downs superpose the components according to their Eqs.(1) and (1a). The researchers performed a nonlinear least-squares model fitting of equation (1) to the data.

The parameters obtained by the decomposition are used for modelling the emission. “During the model fitting, it became clear that the *tails of the*

components deviate slightly from Gaussians. Though they are too small to affect noticeably the pulse profile fits, the *deviations affect* the resultant position angles on the leading edge of the pulse profiles. This is because the intensity ratios determine the position angle at each pulse-longitude” (Krishnamohan and Downs, 1983, see the definition of the position angle therein).¹ In conclusion, we have tails which are not Gaussians. Being not Gaussians, it means that they are power-law tails and therefore q-Gaussians are perfect for investigation.

Here we consider the decomposition of some pulsar profiles at different frequencies. For the decomposition we use software Fityk by Wojdyr, 2010. The specific case considered is that of the profiles of J1022+1001, given by the EPN Database of Pulsar Profiles. We try to maintain the number of components limited to five or six (see [Sparavigna, 2024](#), for reasons). In Fityk processing, we used the Levenberg–Marquardt and the Praxis methods for fitting. We decided to propose, of the two methods, the decomposition with is giving the lower WSSR.

Interference mitigation

Before decompositions, let us add what Bassa et al., 2016, are telling about the “interference mitigation”. “In case of significant radio frequency interference (RFI), [Bassa and coworkers] have implemented two methods to clean the data. ... The first form of RFI-mitigation consists of selecting and masking frequency channels that contain narrow-band RFI. ... A second technique can be applied to data containing time-varying RFI, or broadband RFI”. The method distinguishes RFI “on the premise that *non-Gaussian* amplitudes are caused by RFI”. “The amplitudes of RFI-contaminated samples are replaced by artificial Gaussian noise with the same variance as nearby samples, in order to maintain a constant noise level in the correlated amplitudes regardless of the number of telescopes contributing to each sample” (Bassa et al., 2016). Then the *non-Gaussian* amplitudes are ruled out. So, once more, it is relevant to investigate decompositions in Gaussians and q-Gaussians.

Condon and Ransom, 2016, remembering the first pulsar discovery in 1967, stress it as a “warning against overprocessing data before looking at them, ignoring unexpected signals”. “As radio instrumentation and data-processing software become more sophisticated, more data are “cleaned up” automatically before they reach the astronomer. Matched filtering that brings out the expected signal usually suppresses the unexpected”. That is, non-Gaussian signals are suppressed in the creation of the

¹ About the leading edge, in a discussion by [R. I. Grynko](#), we can see an [image](#) illustrating it for a pulse with a Gaussian temporal profile. The pulse has an “increasing intensity (positive slope) near its leading edge, and a decreasing intensity (negative slope) near the trailing edge”.

pulsar profiles.

Regardless of whether q-Gaussians can be considered attractors or not, are q-Gaussians decompositions different from Gaussians decompositions? Here in the following some examples.

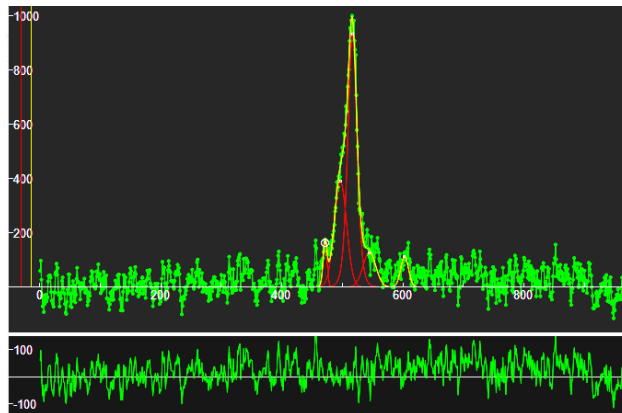


Fig. 1

Profiles of J1022+1001

Let us start from the profile at [4850 MHz](#). Data courtesy Kijak et al., 1997. The data are given in the Figure 1.

The figures that we are here proposing are screenshots of Fityk software. Data are given in green. The Gaussian or q-Gaussian components are given as red lines. The sum of the components is the yellow line. The lower part of the figure is showing the misfit, that is the difference between green data and the yellow line. In the Figure 1, we show all the data. From now on, only the part relevant to the profile is given.

In the Fig.2 (left), five q-Gaussians have been used. [WSSR](#) (weighted sum of squared residuals) is equal to 469767. From left to right the q-parameters are: 0.9999, 0.9992, 1.2166, 0.9992, and 0.9998. In fact, we have four Gaussians, but the main component is a q-Gaussian, with 1.2166. Let us change it into a Gaussian. The decomposition is given in the Fig.2 (right). WSSR is equal to 469803. It seems the attractors are Gaussian functions.

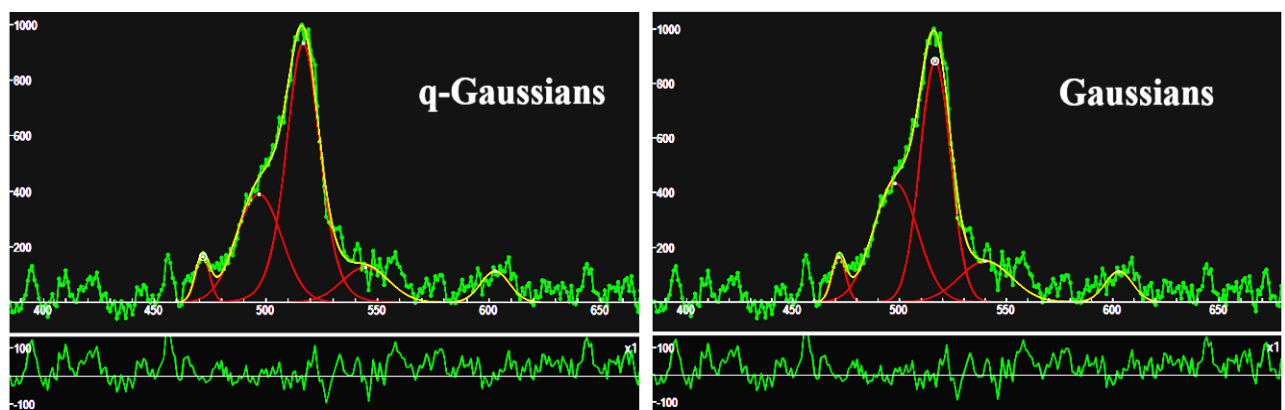


Fig.2 – 4850 MHz Pulsar Profile of J1022+1001 decompositions.

Let us pass to the profile at [3100 MHz](#). Data courtesy Dai et al., 2015. In the Figure 3 (left), the decomposition is given using five q-Gaussians. WSSR is equal to 23.67. From left to right the q-parameters are: 1.1151, 1.3319, 1.3131, 1.1456, and 1.0096. Let us change the components into Gaussians. The decomposition is given in the Fig.3 (right). WSSR is equal to 25.38. Here we have the decomposition with q-Gaussians which has a lower WSSR value. However, the fits could be improved adding further components in both decompositions. Note that the two central components are rather different in the two decompositions.

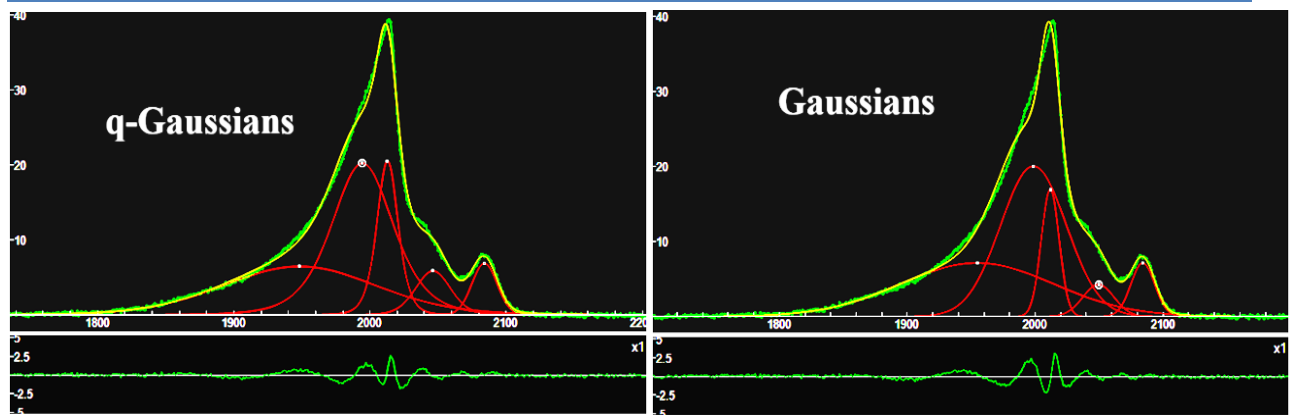


Fig.3 - 3100 MHz Pulsar Profile of J1022+1001 decompositions. The two decompositions are different in the central part.

In the Figure 4 we consider the profile at [1443 Mhz](#). Data courtesy Kramer et al., 1998. In the Fig.4 (left), five q-Gaussians have q-parameters (from left to right): 1.0653, 1.0322 (large component), 1.4000 (small component), 0.9999, and 1.06531. WSSR 0.03390. In the Fig.4 (right), WSSR 0.03607. Note that in the q-Gaussian decomposition, only the smallest component has a q value quite larger than 1.

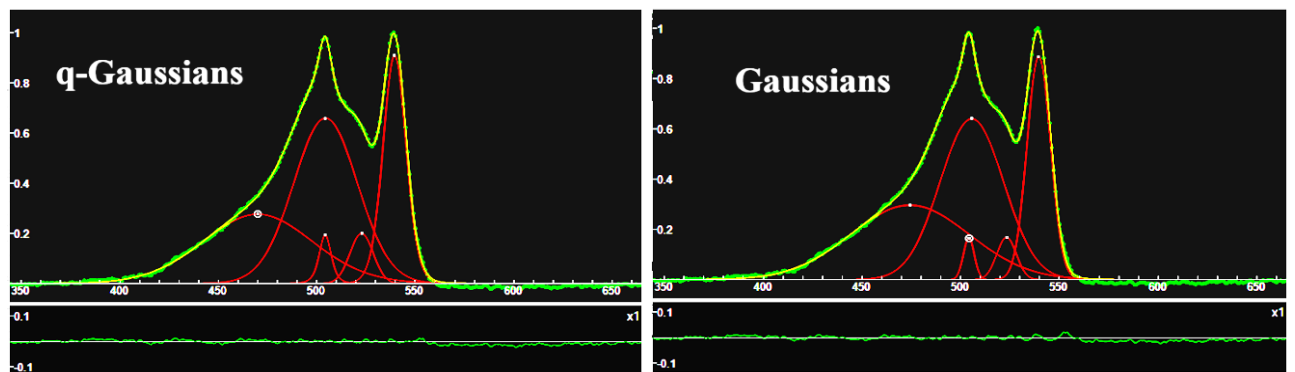


Fig.4 - 1443 MHz Pulsar Profile of J1022+1001 decompositions. Note that, on the right, the data are below the baseline. Therefore, we consider adjusting the baseline as in the following Fig.5.

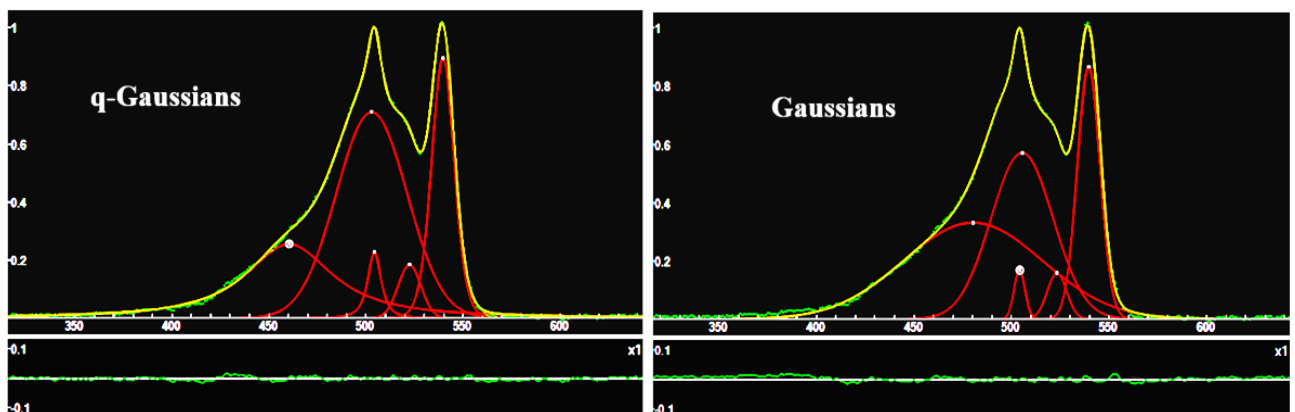


Fig.5 – 1443 MHz profile with baseline correction. Note that the leading edge and the central components are quite different. In fact, in the q-Gaussian decomposition, the leading-edge component has a q parameter equal to 1.89, clearly indicating a power-law behavior of the tail.

In the case given in the Figure 4, we have the occasion to adjust the baseline. The result is given in the Figure 5 for the decomposition in q-Gaussians (on the left, WSSR is 0.0292, the leftmost component has q equal to 1.89) and Gaussians (on the right, WSSR is 0.0491). Let us pass to the profile at [1414 MHz](#). Courtesy Stairs et al., 1999. In the Figure 6, on the left, the q-Gaussians have parameters 1.4563, 1.4265, 0.9998, 1.2750 (WSSR 0.2315). On the

right, the Gaussian decomposition has WSSR equal to 0.2394.

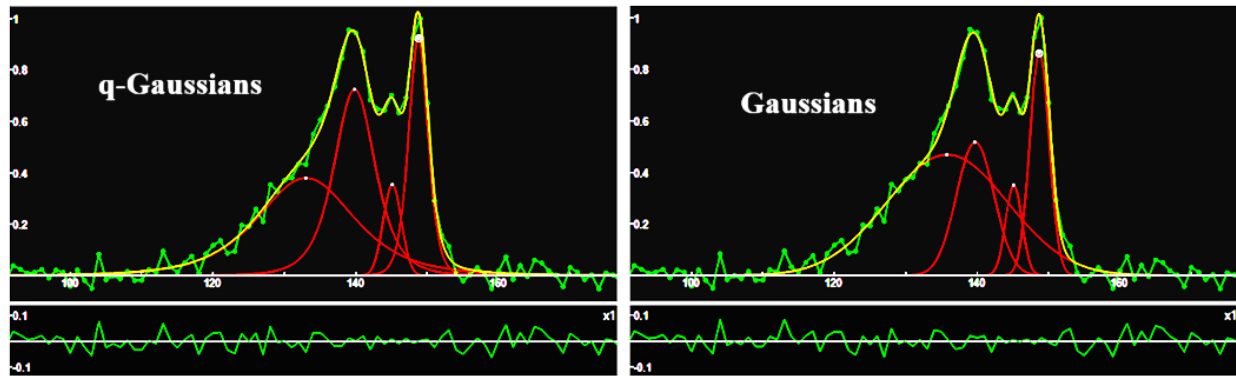


Fig.6 - 1414 MHz Pulsar Profile of J1022+1001 decompositions. Note the different tails of the leading edges. The following Figure 7 is giving the q-Gaussian decomposition of the profile at [1392.5 MHz](#) . Data courtesy Wahl et al., 2023.

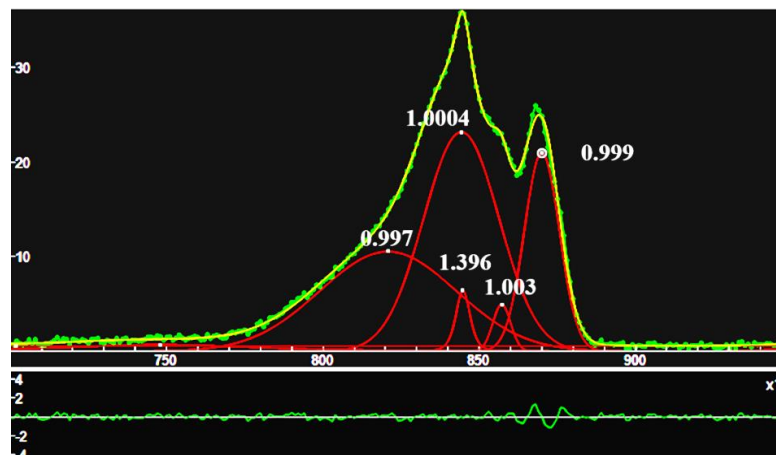


Fig.7 – 1392.5 MHz Pulsar Profile of J1022+1001 q-Gaussian decomposition. The values of the q -parameters are given in the figure. Only one component is different from a Gaussian. It is the same component as in the Figure 4. However, it seems that the baseline needs to be adjusted, because we must add a further leading small component on the left (with center at about 750 in the figure).

In the Figure 8, the profile at [1369 MHz](#) is given. Courtesy Dai et al., 2015. Note the presence of a small quasi-Lorentzian component.

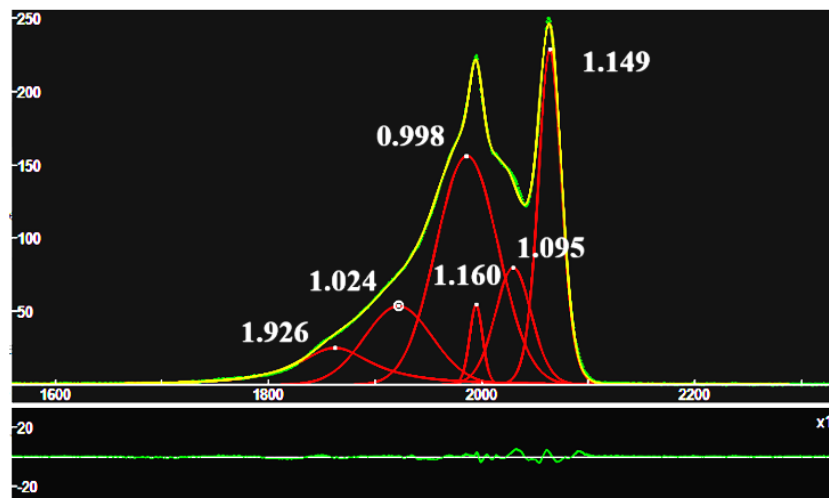


Fig.8 – 1369 MHz Pulsar Profile of J1022+1001 q-Gaussian decomposition. The values of the q -parameters are given in the figure. Note the presence of a quasi-Lorentzian leading-edge component.

In the Figure 9, we are giving the profile at [728 MHz](#). Data courtesy Dai et al., 2015.

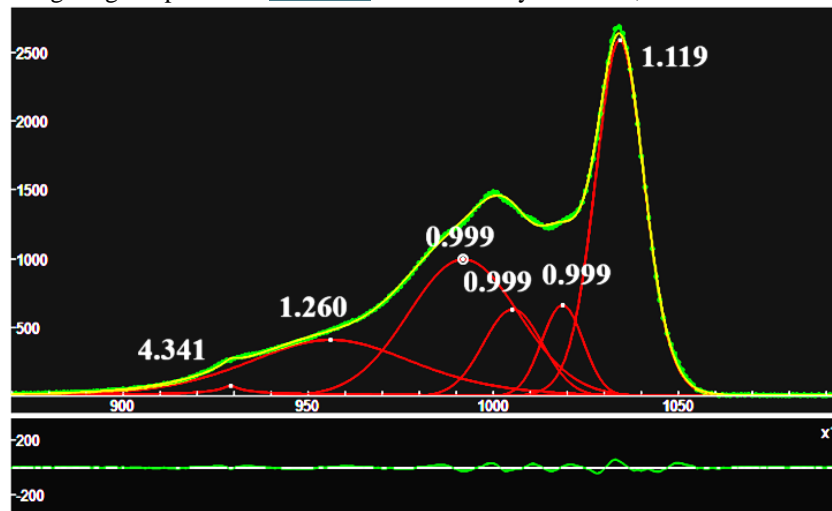


Fig.9 – 728 MHz Pulsar Profile of J1022+1001 q-Gaussian decomposition. The values of the q -parameters are given in the figure.

The Figure 10 is showing the profile at [610 MHz](#). Data courtesy Stairs et al., 1999.

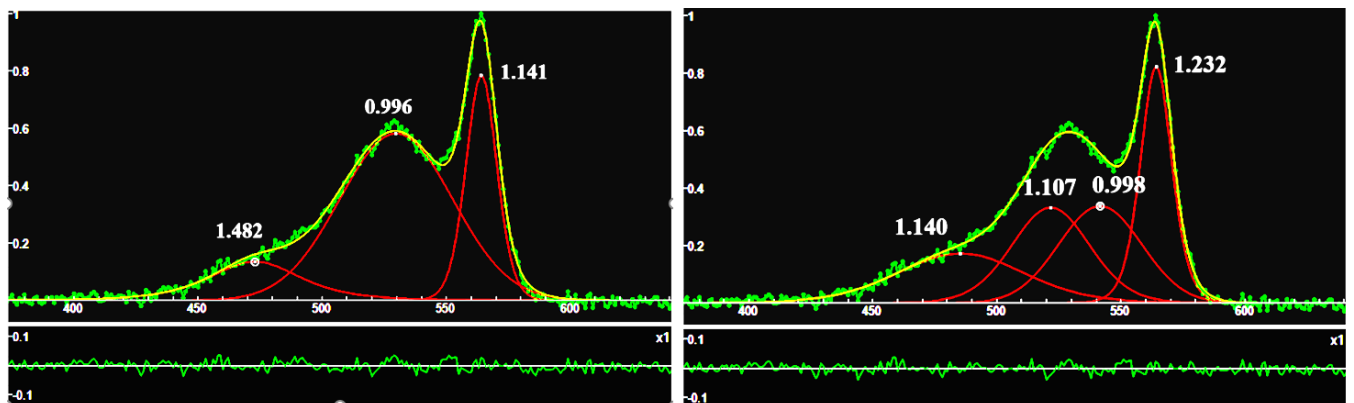


Fig.10 – 610 MHz Pulsar Profile of J1022+1001 q-Gaussian decomposition. The values of the q -parameters are given in the figure. On the left: three q -Gaussians. Note that, due to the band of the misfit, it is a nonsense to add further components (it is better to avoid overfitting). However, if we observe the [plot at the web page of EPN](#), we note that the L curve could be decomposed in more components. Then, let us try to add a further component to the proposed q -Gaussian decomposition. On the right, the data are fitted to four q -Gaussians. The misfit does not change. We can stress what is well-known is Raman spectroscopy, that the decomposition of spectra depends on the number of components and on the used line shape (Ferrari and Robertson, 2000, Meier, 2005).

Let us pass to the case of the profile at [430 MHz](#) (Fig.11). Courtesy Camilo et al. 1996. The case of profile at [410 MHz](#) is given in the Fig.12. Courtesy Stairs et al., 1999. In the Figure 13, the profile at [370 MHz](#) is given. Data courtesy Sayer et al., 1997.

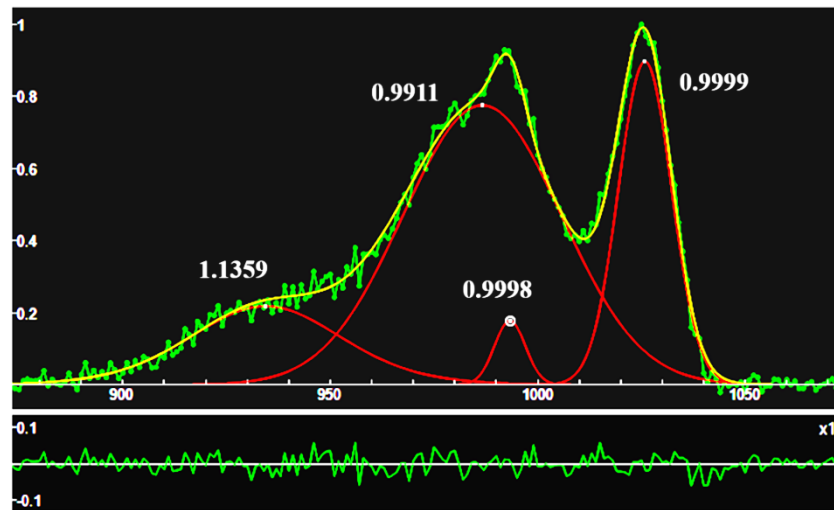


Fig.11 – 430 MHz Pulsar Profile of J1022+1001 q-Gaussian decomposition. The values of the q -parameters are given in the figure. A Gaussian decomposition is giving almost the same result. The only difference is in the power-law of the leading-edge component. The q -parameter is equal to 1.1359

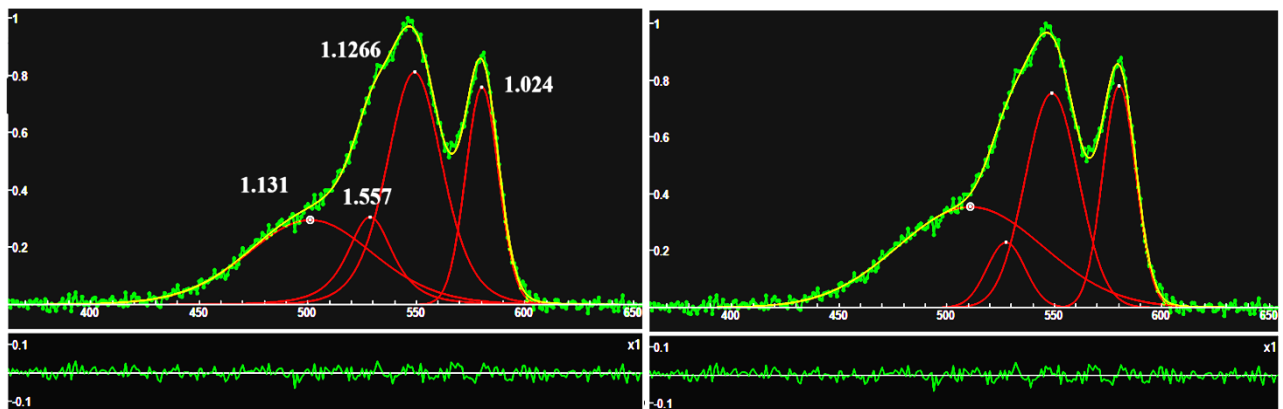


Fig.12 – 410 MHz Pulsar Profile of J1022+1001 q-Gaussian decomposition. On the left: q -Gaussians. The values of the q -parameters are given in the figure. On the right: Gaussian components. A comparison with Fig.11 shows a relevant change in the role of the middle components.

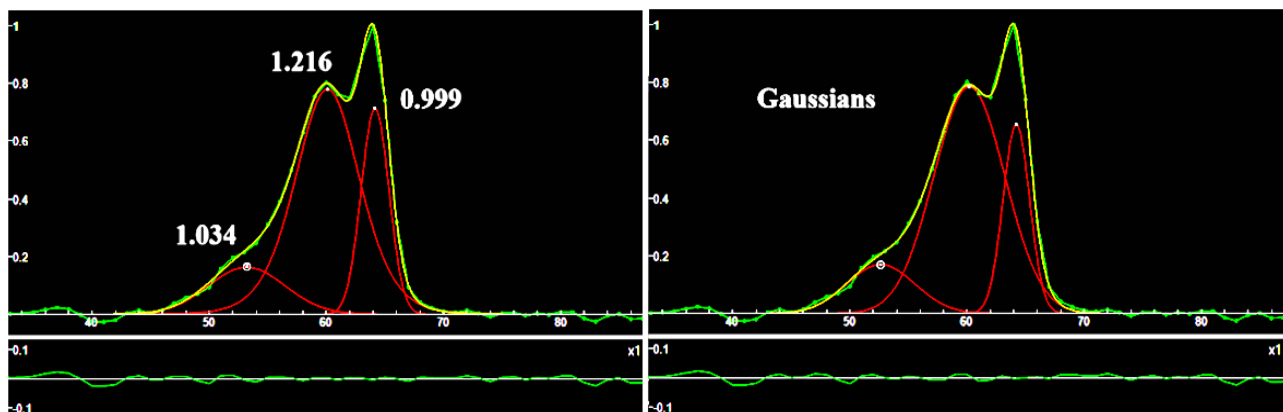


Fig.13 – 370 MHz Pulsar Profile of J1022+1001 q-Gaussian decomposition. On the left: q -Gaussians. The values of the q -parameters are given in the figure. On the right: Gaussian components. Note the presence of an oscillation of the baseline.

The last case that we considered is the profile at [325.9 MHz](#). Data courtesy Wahl et al., 2023.

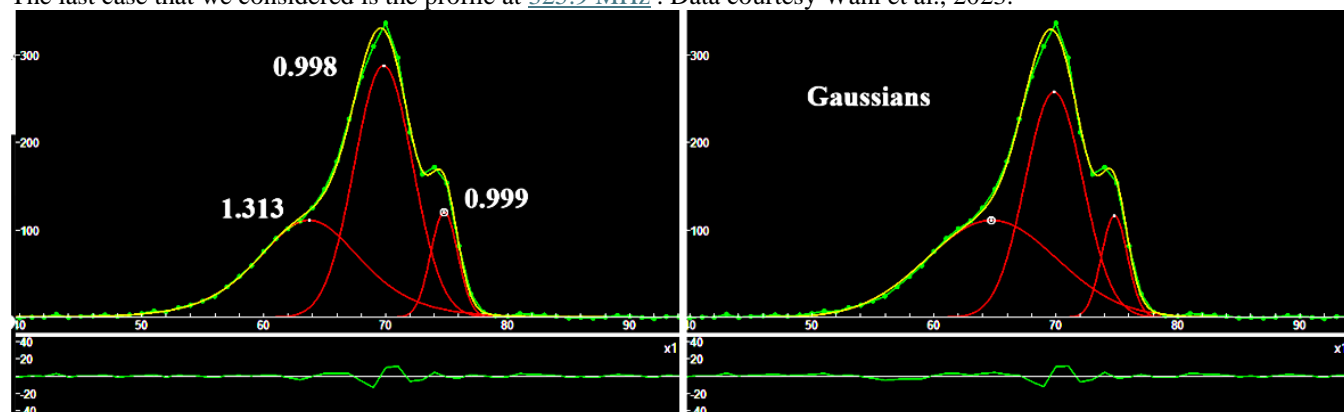


Fig.14 – 325.9 MHz Pulsar Profile of J1022+1001 *q*-Gaussian decomposition. On the left: *q*-Gaussians. The values of the *q*-parameters are given in the figure. On the right: Gaussian components. Also in this case, the leading component has a power-law tail.

Discussion about J1022+1001

In the previously given decompositions of the J1022+1001 profiles we have a variety of cases where the *q*-Gaussians have values of the *q*-parameters close to 1. It means that the *q*-Gaussians are quasi-Gaussian functions. Therefore, we could guess Gaussian attractors for these distributions. However, we have also cases where the *q*-parameter is substantially different from 1. In fact, deviations from the Gaussian behavior of the tails of pulsar profile have been already noted by Krishnamohan and Downs, 1983. Using the *q*-Gaussian functions we can quantify it.

About pulsar J1022+1001, from Padmanabh et al., 2021, we know that it “is a binary pulsar with a spin period of 16.45 ms in a 7.8-day orbit (Camilo et al. 1996) with a white dwarf companion (Lundgren et al. 1996). The average pulse profile exhibits a two peaked structure at 1.4 GHz. The pulsar is currently a part of the European Pulsar Timing Array (EPTA) and the Parkes Pulsar Timing Array (PPTA) among other pulsars in the quest to detect nanohertz gravitational waves”. However, “several studies across many years using different telescopes have shown conflicting results regarding the pulse profile stability of this pulsar” (Padmanabh et al., 2021).

The pulsar J1022+1001 is therefore relevant for the reasons given in Padmanabh et al., 2021. “Millisecond pulsars in timing arrays can act as probes for gravitational wave detection and improving the solar system ephemerides among several other applications. However, the *stability of the integrated pulse profiles* can limit the precision of the ephemeris parameters and in turn the applications derived from it. It is thus crucial for the pulsars in the array to have *stable* integrated pulse profiles”. Padmanabh and coworkers “evidence for long-term profile instability in PSR J1022+1001 ... this intrinsic variability in the pulse shape persists over time scales of years”. The researchers suggest “additional intrinsic effects as the origin for the

variation”. Padmanabh and coworker stress that, to detect gravitational waves in the nanohertz regime, relevant “is the technique of pulsar timing where the arrival time of the pulsar signal is monitored by comparison against a *reference template* of the average pulse profile. Here, typically, tens of thousands of pulses are averaged to form an integrated profile. A template is generated from such integrated profiles across many observations. In order to avoid self-imaging effects (Hotan et al. 2005), the grand average profile is often converted into a template by modelling the pulse as a superposition of multiple Gaussians or von Mises functions. This *noise free template* is then used as a reference and cross correlated with profiles from each epoch to calculate the times of arrival (TOAs)”. Please consider the detailed discussion of the modified Hotan method that the researchers used to investigate the stability of the J1022+1001 profile. About the integrated profiles and templates, see please the discussion at pag.127, in Keane, 2010.

In Hotan et al., it is noted that Gaussians have Fourier transforms, which are Gaussian functions too. Therefore, these functions can be easily used for the elaboration of the signals, and the creation of a final template profile. Then, when we consider pulsar profiles, which have been obtained from the integration of many cycles, we could encounter profiles elaborated as Gaussian templates. Consequently, a decomposition could give just Gaussian results, with the difficulty to find deviation from the Gaussian line shapes. However, in some cases seen above, differences exist. Actually, Krishnamohan and Downs already observed deviations from the Gaussian behavior of the tails.

Acknowledgement

Part of this research has made use of the EPN Database of Pulsar Profiles maintained by the University of Manchester, available at <https://psrweb.jb.man.ac.uk/epndb/>.

References

1. Bassa, C.G., Janssen, G.H., Karuppusamy, R., Kramer, M., Lee, K.J., Liu, K., McKee, J., Perrodin, D.E.L.P.H.I.N.E., Purver, M., Sanidas, S. and Smits, R., 2016. LEAP: the large European array for pulsars. *Monthly Notices of the Royal Astronomical Society*, 456(2), pp.2196-2209.
2. Bianucci, M. (2021). Operators central limit theorem. *Chaos, Solitons & Fractals*, 148, 110961.
3. Breitenberger, E. (1963). Analogues of the normal distribution on the circle and the sphere. *Biometrika*, 50(1/2), 81-88.
4. Camilo, F., Nice, D. J., Shrauner, J. A., & Taylor, J. H. (1996). Princeton-Arecibo Declination-Strip Survey for Millisecond Pulsars. I. *Astrophysical Journal* v. 469, p. 819, 469, 819.
5. Condon, J. J., & Ransom, S. M. (2016). *Essential radio astronomy* (Vol. 2). Princeton University Press.
6. Dai, S., Hobbs, G., Manchester, R.N., Kerr, M., Shannon, R.M., van Straten, W., Mata, A., Bailes, M., Bhat, N.D.R., Burke-Spolaor, S. and Coles, W.A., 2015. A study of multifrequency polarization pulse profiles of millisecond pulsars. *Monthly Notices of the Royal Astronomical Society*, 449(3), pp.3223-3262.
7. Deng, J. (2010, June). Relationship between Lévy Distribution and Tsallis Distribution. In *ICEIS* (2) (pp. 360-367).
8. Fano, U. (1961). Effects of configuration interaction on intensities and phase shifts. *Physical review*, 124(6), 1866.
9. Ferrari, A. C., & Robertson, J. (2000). Interpretation of Raman spectra of disordered and amorphous carbon. *Physical Review B* 61: 14095–14107.
10. Gardner, F. F., & Whiteoak, J. B. (1969). The linear polarization of radio sources between 11 and 20 cm wavelength. II. Polarization and related properties of extragalactic sources. *Australian Journal of Physics*, 22(1), 107-120.
11. Hanel, R., Thurner, S., & Tsallis, C. (2009). Limit distributions of scale-invariant probabilistic models of correlated random variables with the q-Gaussian as an explicit example. *The European Physical Journal B*, 72(2), 263.
12. Helfand, D. J., Manchester, R. N., & Taylor, J. H. (1975). Observations of pulsar radio emission. III-Stability of integrated profiles. *Astrophysical Journal*, vol. 198, June 15, 1975, pt. 1, p. 661-670., 198, 661-670.
13. Hilhorst, H. J. (2009). Central limit theorems for correlated variables: some critical remarks. *Brazilian Journal of Physics*, 39, 371-379.
14. Hilhorst, H. J. (2010). Note on a q-modified central limit theorem. *Journal of Statistical Mechanics: Theory and Experiment*, 2010(10), P10023.
15. Hotan, A. W., Bailes, M., & Ord, S. M. (2005). PSR J0737-3039A: baseband timing and polarimetry. *Monthly Notices of the Royal Astronomical Society*, 362(4), 1267-1272.
16. Keane, E. F. (2010). *The transient radio sky*. The University of Manchester (United Kingdom).
17. Kijak, J., Kramer, M., Wielebinski, R., & Jessner, A. (1997). Observations of millisecond pulsars at 4.85 GHz. *Astronomy and Astrophysics*, v. 318, p. L63-L66, 318, L63-L66.
18. Kramer, M., Wielebinski, R., Jessner, A., Gil, J. A., & Seiradakis, J. H. (1994). Geometrical analysis of average pulsar profiles using multi-component Gaussian FITS at several frequencies. I. Method and analysis. *Astronomy and Astrophysics Suppl.*, Vol. 107, p. 515-526 (1994), 107, 515-526.
19. Kramer, M. (1994). Geometrical analysis of average pulsar profiles using multi-component Gaussian FITS at several frequencies. II. Individual results. *Astronomy and Astrophysics Suppl.*, Vol. 107, p. 527-539 (1994), 107, 527-539.
20. Kramer, M., Xilouris, K.M., Lorimer, D.R., Doroshenko, O., Jessner, A., Wielebinski, R., Wolszczan, A. and Camilo, F., 1998. The characteristics of millisecond pulsar emission. I. Spectra, pulse shapes, and the beaming fraction. *The Astrophysical Journal*, 501(1), p.270.
21. Krishnamohan, S., & Downs, G. S. (1983). Intensity dependence of the pulse profile and polarization of the VELA pulsar. *Astrophysical Journal*, Part 1, vol. 265, Feb. 1, 1983, p. 372-388., 265, 372-388.
22. Lundgren, S. C., Foster, R. S., & Camilo, F. (1996, January). Hubble Space Telescope Observations of Millisecond Pulsar Companions: Constraints on Evolution. In *International Astronomical Union Colloquium* (Vol. 160, pp. 497-500). Cambridge University Press.
23. Mantegna, R. N., & Stanley, H. E. (1999). *Introduction to econophysics: correlations and complexity in finance*. Cambridge university press.
24. Marsh, J. A., Fuentes, M. A., Moyano, L. G., & Tsallis, C. (2006). Influence of global correlations on central limit theorems and entropic extensivity. *Physica A: Statistical Mechanics and its Applications*, 372(2), 183-202.
25. Meier, R. J. (2005). On art and science in curve-fitting vibrational spectra. *Vibrational spectroscopy*, 2(39), 266-269.
26. Naudts, J. (2009). The q-exponential family in statistical physics. *Central European Journal of Physics*, 7, 405-413.
27. Osłowski, S., van Straten, W., Hobbs, G. B., Bailes, M., & Demorest, P. (2011). High signal-to-noise ratio observations and the ultimate limits of precision pulsar timing. *Monthly Notices of the Royal Astronomical Society*, 418(2), 1258-1271.
28. Padmanabh, P. V., Barr, E. D., Champion, D. J., Karuppusamy, R., Kramer, M., Jessner, A., & Lazarus, P. (2021). Revisiting profile instability of PSR J1022+ 1001. *Monthly Notices of the Royal Astronomical Society*, 500(1), 1178-1187.
29. Sayer, R. W., Nice, D. J., & Taylor, J. H. (1997). The Green Bank northern sky survey for fast pulsars. *The Astrophysical Journal*, 474(1), 426.
30. Sparavigna, A. C. (2024). q-Gaussian and q-BWF Functions Applied to the Decomposition of Pulsar Profiles: Preliminary Results, *International Journal of Sciences* 06(2024):1-9 DOI: 10.18483/ijSci.2768
31. Sparavigna, A. C. (2023). Convolution and Fourier Transform: from Gaussian and Lorentzian Functions to q-Gaussian Tsallis Functions. *Int. J. Sciences*, 11, 7-11.
32. Stairs, I. H., Thorsett, S. E., & Camilo, F. (1999). Coherently dedispersed polarimetry of millisecond pulsars. *The Astrophysical Journal Supplement Series*, 123(2), 627.
33. Tsallis, C. (1988). Possible generalization of Boltzmann-Gibbs statistics. *Journal of statistical physics*, 52, 479-487.
34. Tsallis, C. (2011). The nonadditive entropy S_q and its applications in physics and elsewhere: Some remarks. *Entropy*, 13(10), 1765-1804.
35. Umarov, S., Tsallis, C., Steinberg, S. (2008). On a q-Central Limit Theorem Consistent with Nonextensive Statistical Mechanics. *Milan J. Math. Birkhauser Verlag*, 76: 307–328. doi:10.1007/s00032-008-0087-y. S2CID 55967725.
36. Van der Wateren, E., Bassa, C.G., Cooper, S., Griebmeier, J.M., Stappers, B.W., Hessels, J.W.T., Kondratiev, V.I., Michilli, D., Tan, C.M., Tiburzi, C., & Weltevrede, P. (2023). The LOFAR Tied-Array All-Sky Survey: Timing of 35 radio pulsars and an overview of the properties of the LOFAR pulsar discoveries. *Astronomy & Astrophysics*, 669, p.A160.
37. Wahl, H., Rankin, J., Venkataraman, A., & Olszanski, T. (2023). Radio pulsar emission-beam geometry at low frequency: LOFAR High-Band Survey sources studied using Arecibo at 1.4 GHz and 327 MHz. *Monthly Notices of the Royal Astronomical Society*, 520(1), 314-321.
38. Wojdyr, M. (2010). Fityk: a general-purpose peak fitting program. *Journal of Applied Crystallography*, 43(5-1), 1126-1128.